

# Catalytic Properties of Sn–Ce–Rh–O in Dehydrogenation and Oxidative Dehydrogenation Reactions<sup>1</sup>

R. Klimkiewicz<sup>a</sup>, H. Teterycz<sup>b</sup>, E. Sikora<sup>c</sup>, G. S. Szymański<sup>d</sup>, and J. Trawczyński<sup>e</sup>

<sup>a</sup> Institute of Low Temperature and Structure Research, Polish Academy of Sciences, Wrocław, Poland

e-mail: R.Klimkiewicz@int.pan.wroc.pl

<sup>b</sup> Faculty of Microsystem Electronics and Photonics, Wrocław University of Technology, Wrocław, Poland

<sup>c</sup> Institute of Organic Chemistry and Technology, Kraków University of Technology, Kraków, Poland

<sup>d</sup> Faculty of Chemistry, Copernicus University, Toruń, Poland

<sup>e</sup> Institute of Chemistry and Technology of Petroleum and Coal, Wrocław University of Technology, Wrocław, Poland

Received January 26, 2005

**Abstract**—A new, single-phase  $\text{Sn}_{0.925}\text{Ce}_{0.07}\text{Rh}_{0.005}\text{O}_2$  gas sensitive material has up to now been used as a catalyst for the bimolecular condensation of aldehydes and C-alkylation of hydroxyarenes with alcohols. It was subjected to the isopropanol test, the oxidative dehydrogenation of cyclohexane test, and the cyclohexene +  $\text{H}_2$  test. A general physico-chemical analysis was done, and it included XRD, SEM, mercury porosimetry, TPD  $\text{NH}_3$ , and IR (pyridine) spectroscopy. The tests results are compliant with the basic character of the catalyst; however, it reveals significant total acidity (0.274 mmol  $\text{NH}_3/\text{g}$ ) and the presence of Lewis strong acid centers (0.126 mmol Py/g). The presence of these centers in the dehydrogenating catalysts cause the ability to catalyze both the bimolecular condensation of aldehydes and C-alkylation of hydroxyarenes with alcohols.

**DOI:** 10.1134/S0023158407010107

## INTRODUCTION

Oxide catalytic materials as well as the effects typical for heterogeneous catalysis may be found useful in sensor technology. The properties of resistive chemical gas sensors are similar to those of heterogeneous catalysts. Both the type and state of the surface along with the material microstructure form these properties. The resistance change observed during gas detection results from the heterogeneous catalytic reactions ongoing on the surface of the gas-sensitive material and strongly depends on the concentration of the detected gas compounds. These analogies suggest taking the materials developed originally for gas sensing and applying them as heterogeneous catalysts.

By the end of the last decade, a new single-phase gas sensitive material had been developed— $\text{Sn}_{0.925}\text{Ce}_{0.07}\text{Rh}_{0.005}\text{O}_2$  [1]. This n-type semiconductive material reveals anomalous features during gas detection ( $\text{CO}$ ,  $\text{CH}_4$ ,  $\text{C}_2\text{H}_5\text{OH}$ ) [2]. Due to the fast and stable response, gas sensors on the basis of this material may be applied in electronic noses. Later, the material, originally developed for gas sensing applications, was used as a heterogeneous catalyst for primary alcohol conversions. The tin and cerium oxides applied to the described material are basic oxides (rhodium is zero-valent [2]). Moreover, the  $\text{CO}_2$  chemisorption measurements revealed that on the binary system  $\text{Sn}_{0.93}\text{Ce}_{0.07}\text{O}_2$

there are more basic centers than on single oxides  $\text{SnO}_2$  and  $\text{CeO}_2$  [3]. Thus, the catalyst should be dehydrogenative for alcohols [4]. The experimental application of  $\text{Sn}_{0.925}\text{Ce}_{0.07}\text{Rh}_{0.005}\text{O}_2$  for primary alcohol conversions have shown, however, that the material catalyzes the consecutive bimolecular condensation of aldehydes very selectively, with high ketone yield [5]:



$\text{Sn}_{0.925}\text{Ce}_{0.07}\text{Rh}_{0.005}\text{O}_2$  was also found to be an active and ortho-selective catalyst for the C-alkylation of hydroxyarenes with alcohols [6]. In the gas phase of phenol methylation, a summarized selectivity to *ortho*-cresol and 2,6-xylol at 643 K reached 93% at the 71% conversion of phenol, while O-alkylation was an insignificant process.

The present research results reveal that the same catalysts may be applied for both the bimolecular condensation of primary alcohols and alcohol alkylation of hydroxyarenes (e.g., iron oxide cited in [6]). The reason is that both reactions have a competitive character. In the case of the alkylation of hydroxyarenes with higher primary alcohols, the competitive activity of the condensation reaction of these alcohols to ketones is observed [7]. In the case of the ketonization of primary alcohols, the ketones tend to alkylate to molecules of higher carbon atom contents [8]. The Tishchenko reaction reversibility provides for the application of bimo-

<sup>1</sup> The article was submitted by the authors in English.

lecular condensation of aldehydes and also ketonization of esters. The catalyst containing the oxides of Sn, Ce, and Rh was employed in such a transformation of esters, and the mechanism of this transformation was investigated [9]. It was also applied for the utilization trial by ketonization of a mixture of methyl esters of fatty acids resulting from transesterification of postindustrial oil [10].

Taking into account the anomalous features of this material detected in the context of sensor technology and along with its good catalytic properties in the above reactions, the authors decided to subject it to accessory physical and chemical investigation. Tin dioxide was also investigated for the sake of comparison.

## 2. EXPERIMENTAL

### 2.1. Synthesis

Tin dioxide was synthesized with the modified Okazaki method [11, 12]. Dehydrated tin (IV) chloride (Fluka p.a.) was dissolved in glacial acetic acid (Fluka p.a.) and poured into a huge amount of hot deionized water (353 K). As the result of hydrolysis, a fine-grained hydrated tin dioxide was precipitated. The precipitate was washed from the chloride ions, dried (323 K), and calcined at the temperature of 873 K.

The final 3-component  $\text{Sn}_{0.925}\text{Ce}_{0.07}\text{Rh}_{0.005}\text{O}_2$  material was obtained with coprecipitation of tin and cerium dioxides, which were then impregnated by a hydroalcoholic solution of rhodium chloride [1, 5]. The  $\text{SnO}_2$  and  $\text{CeO}_2$  precipitate was precipitated from the water solution of tin (IV) chloride and ammonia-cerium nitrate (Fluka p.a.) using a 3 N solution of ammonia. The precipitate was washed with deionized water several times to remove the chloride ions. The resulting precipitate, free of chloride ions, was washed with propan-2-ol and dried at 323 K. The dried precipitate was impregnated with a rhodium chloride (Fluka p.a.) solution, washed with the propan-2-ol solution, dried again, and calcined at 873 K.

### 2.2. Characterizations

**2.2.1. Physical.** The study of the crystallographic structure of the powders was performed with X-ray diffraction using the Materials Research Diffractometer by Philips ( $\text{CuK}_\alpha$  radiation). The microstructure of the catalyst powders was checked before and after the catalysis process using the scanning electron microscope JSM 5800 LV by Jeol. The microscope was equipped with the X-ray microanalysis system Oxford ISIS 300, with a semiconductor detector analyzing the energy of the characteristic X-ray radiation. The distribution of the elements in the near-surface layer was estimated with the X-ray microprobe. The specific sur-

face was determined using the measurements of mercury porosimetry obtained from the Pascal 440 porosimeter.

### 2.2.2. Acidity type and acidity strength distribution.

The specific acidity and acidity strength distribution of the studied materials as a function of the ammonia desorption temperature were evaluated by the method of temperature-programmed desorption of ammonia ( $\text{NH}_3$  TPD) according to the following procedure: heating of the sample ( $\sim 2$  g) at 823 K under argon atmosphere during 1 h, cooling in an argon stream to the temperature of 453 K, adsorption of pure ammonia at 453 K for 0.5 h, purging with argon at 453 K for 1 h in order to remove physically adsorbed ammonia, and TPD measurement (argon stream heating rate of 10 K/min, temperature range from 453 to 823 K). The concentration of desorbed ammonia was measured by a thermal conductivity detector. For quantitative analysis, the apparatus was first calibrated with the empty reactor. The relative experimental error of TPD measurements was found to be less than 3%. The results of TPD experiments were worked out according to the methodology described elsewhere [13].

The concentration of the Lewis centers on the sample surface was measured by means of IR spectroscopy according to a procedure described in literature [14] using pyridine as a test molecule. IR spectra were recorded at room temperature with a SPECORD M80 grating spectrometer. Self-supporting wafers (ca. 10 mg) were calcined in air at 773 K in the IR cell.

The vacuum-proof cell was evacuated, and wafers were exposed to pyridine vapors ( $T = 298$  K,  $p = 939$  Pa,  $t = 36$  min), then evacuated at 423 K for 90 min.

**2.2.3. Isopropanol test.** The propan-2-ol test was carried out in a fixed-bed flow microreactor working on-line with gas chromatograph (equipped with FID), in the temperature range 473–573 K, under atmospheric pressure. Argon was used as an inert gas ( $Q_{\text{Ar}} = 360 \text{ cm}^3/(\text{cm}^3 \text{ Cat h})$ ). The alcohol was fed as a liquid by a micropump to the top of the microreactor (flow rate of propan-2-ol was  $Q_{i\text{-Pr}} = 4.1 \text{ cm}^3/\text{h}$ ). Next, the reactant was vaporized in the preheated reactor section and mixed homogeneously with argon.

The microreactor was packed with  $1.0 \text{ cm}^3$  of catalyst (fraction of 0.2–0.3 mm grain size). Before each of the catalytic cycles, the catalyst was activated at 723 K in air for 2 h. Next, it was conditioned in the carrier-gas atmosphere and then cooled to the reaction temperature.

The GC analysis of the products was carried out with a programmed temperature increase, in the range 353–433 K, on a Porapak-Q packed column (the column length = 1 m). The first sample of the products was analyzed after the first 15 min of the process.

**2.2.4. Cyclohexane test.** The oxidative dehydrogenation of cyclohexane was investigated in a fixed bed flow-type microreactor working under atmospheric pressure. The air stream ( $8 \text{ cm}^3/\text{min}$ ) was saturated with cyclohexane vapors at 290 K. The catalytic tests were conducted in the temperature range of 473–633 K using 200 mg of catalyst. The GC on-line analysis of the product was performed at 353 K with a Chromatron GCHF 18.3 chromatograph equipped with stainless column (length: 3 m, inner diameter = 4 mm) containing Carbowax 20M (10%) on Chromosorb WAW 80/100 mesh and FID detector using nitrogen as a carrier gas. In addition, the gaseous products were also analyzed by IR method. Prior to the catalytic tests, the samples placed in the microreactor were conditioned in a helium stream at 473 K for 2 h.

**2.2.5. Cyclohexene +  $\text{H}_2$  test.** The experiments were conducted in a gradientless microreactor with an internal recycle flow system. 1  $\text{cm}^3$  of a sample was used with a flow of 4.8  $\text{dm}^3/\text{h}$  of a feed containing 2.5% vol. cyclohexene in hydrogen. Standard experiments were performed at atmospheric pressure and temperatures between 470 and 685 K.

Composition of the reaction products was determined on-line using GC “AutoSystem XL” (Perkin Elmer) equipped with FID and N931-6090 PE-5 capillary column ( $d = 0.32 \text{ mm}$ ,  $l = 60 \text{ m}$ ) containing 5% phenyl on methylpolysiloxane. The gas chromatographic separations were carried out at 323 K. Conversion of cyclohexene and yields of the products of cyclohexene hydrogenation, isomerization, and ring opening were determined.

### 3. RESULTS AND DISCUSSION

The dopants were added to the pure  $\text{SnO}_2$  in the early stages of preparation. They modified the crystallographic structure; specific surface; porosity; and, importantly, the kind and the quality of the surface active centers. Additionally, the variable valence dopants could significantly increase the ability of the original materials to store oxygen [15]. It is connected with the fact that the temperature of the reduction of the solid-state oxide solution is significantly lower than that of the pure oxide. This is caused by significant modification of the oxide subnet around the dopant cation as well as creation of the mobile oxygen ion responsible for the increased reducibility [16].

Pure tin (IV) oxide is an effective catalyst neither for bimolecular condensation of *n*-butanol [5] nor for methanol alkylation of phenol [6].

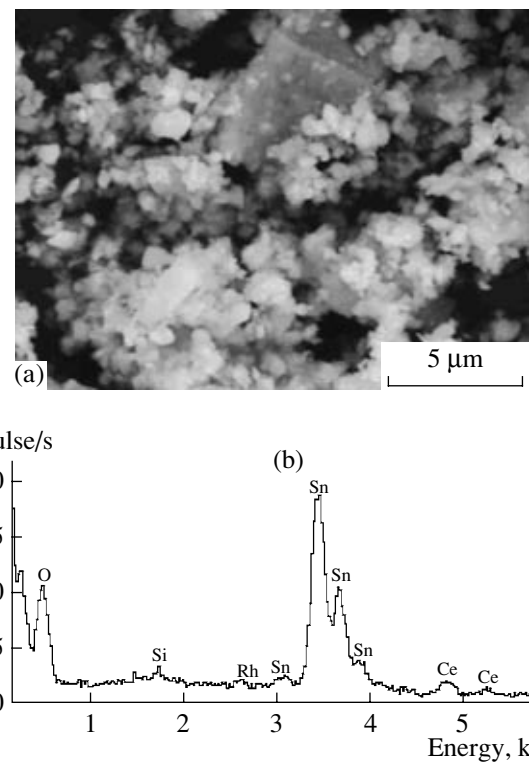


**Fig. 1.** Microstructure of the single-phase three component catalyst powder (a) and composition of the elements, estimated using an X-ray microprobe (b).

#### 3.1. General Characteristics of $\text{Sn}_{0.925}\text{Ce}_{0.07}\text{Rh}_{0.005}\text{O}_2$

The X-ray investigation of the tin dioxide powder fabricated with the modified Okazaki method revealed its rutile crystallographic structure. The coprecipitated tin and cerium dioxides doped with rhodium formed the single-phase system with a rutile crystallographic structure as well [2]. However, adding cerium caused an increase in the parameters of the lattice. The lattice parameters for the synthesized  $\text{SnO}_2$  were  $a = 4.739 \text{ \AA}$ ,  $c = 3.188 \text{ \AA}$ , while for  $\text{Sn}_{0.925}\text{Ce}_{0.07}\text{Rh}_{0.005}\text{O}_2$  composition, they were  $a = 5.309 \text{ \AA}$  and  $c = 3.552 \text{ \AA}$ . The average size of the crystallites was also estimated (Debye-Scherrer method)—246 nm for the tin dioxide powder and 70 nm for the composition.

The microscopic observations were in agreement with the results obtained with the X-ray diffractometer and revealed that the powder of the triple oxide is made of conglomerates of crystallites (Fig. 1). The element distribution, i.e., tin and cerium, was found to be homogeneous for the whole surface of the investigated sample.

The total volume of the pores determined with the mercury porosimetry method was equal to  $0.093 \text{ cm}^3/\text{g}$  while the average pore radius was 8.1 nm (Fig. 2). The bulk density (including pores) was equal to  $1.97 \text{ g}/\text{cm}^3$ , and the apparent density (including only micropores)

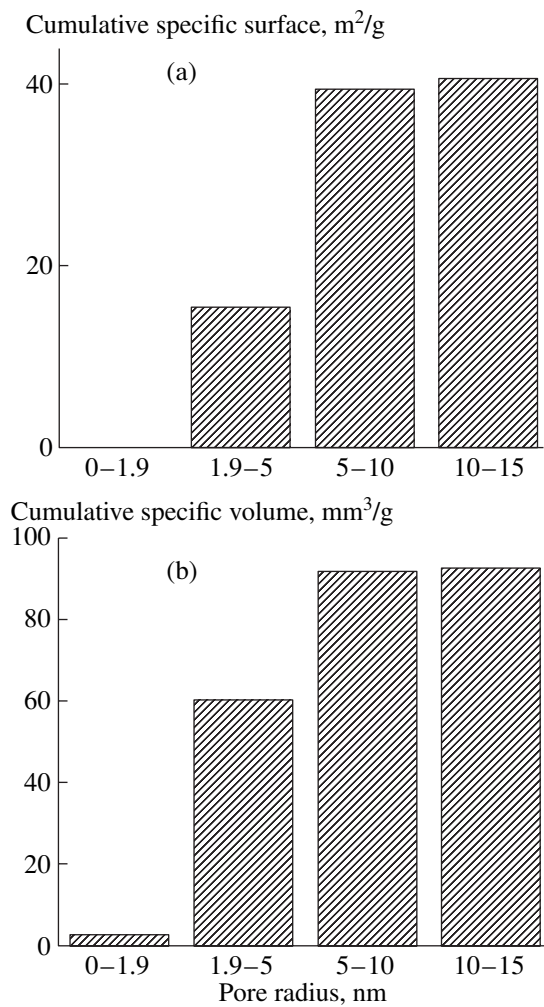


**Fig. 2.** Specific surface (a) and specific volume (b) versus pore size distributions of  $\text{Sn}_{0.925}\text{Ce}_{0.07}\text{Rh}_{0.005}\text{O}_2$ .

was equal to 2.4  $\text{g}/\text{cm}^3$ . The total specific surface was equal to  $40.6 \text{ m}^2/\text{g}$ .

### 3.2. Acid Properties

The oxides from  $\text{Sn}_{0.925}\text{Ce}_{0.07}\text{Rh}_{0.005}\text{O}_2$  reveal strong basic properties [4]; however, investigation of

Temperature range	453–523	523–573	573–623	623–673	673–723	723–773	773–823
Percentage	1.4	10.2	14.6	16.0	15.7	19.7	22.3

It was revealed by means of IR spectroscopy that, on the surface of the sample, there were no acidic centers of the Brønsted type (absence of  $1540 \text{ cm}^{-1}$  band). The concentration of Lewis acid centers was measured (for the band at  $1450 \text{ cm}^{-1}$ ) to be equal to 0.126 mmol Py/g. The observed discrepancy between the amounts of acid

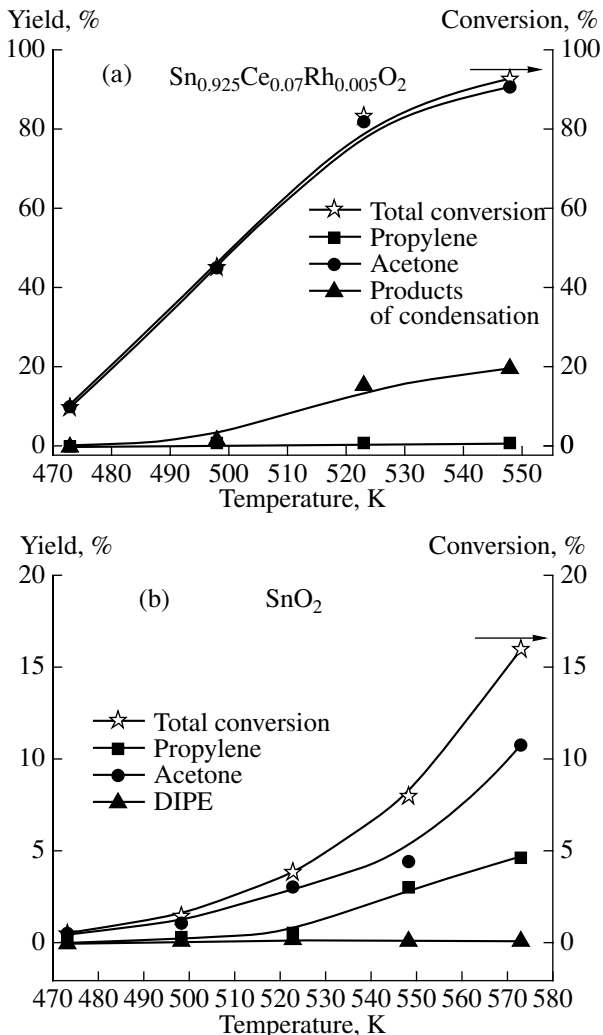


**Fig. 3.** Conversion and yield of acetone and propylene revealed by the isopropanol test performed on the investigated materials.

the temperature programmed desorption has shown a significant amount of acid centers on the surface and the different acid strengths of the centers. The total acidity of the sample was 0.274 mmol  $\text{NH}_3/\text{g}$ . The acidity strength distribution (percentage of desorbed ammonia) was as follows:

sites determined from ammonia and pyridine adsorption can be the result of microporosity of the material and of different base strengths. It is likely that pyridine can adsorb only on the sites with the highest acid strength. This result is in agreement with other physico-chemical investigations of the material [17].

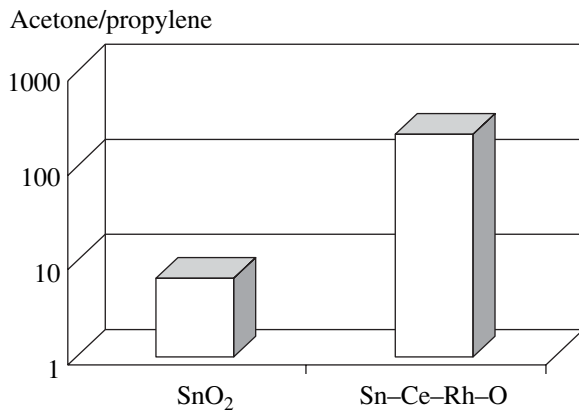


**Fig. 4.** Acetone to propene ratio of the tin dioxide and cerium-rhodium doped tin dioxide.

### 3.3. Isopropanol Test

The isopropanol test revealed that the activity of the three-component tin-cerium-rhodium catalyst is much higher than that for pure tin dioxide (Figs. 3a, 3b). The catalyst also showed a very high dehydrogenating selectivity. In the whole range of the temperature, the acetone dominates as a reaction product and, for the higher temperatures, the products of acetone condensation appear in addition—mainly mesityl oxide arising from it.

The isopropanol activity is much higher than that for the primary alcohols because of the higher stability of the second order carbocation, which easily arises from isopropanol dehydration. Concerning tin dioxide, for isopropanol conversion higher than *n*-butanol conversion, besides dehydrogenation, dehydration to diisopropyl ether and propene also took place. This confirms that the tin dioxide donation with cerium and rhodium caused a strong increase in the dehydrogenating function at the expense of the dehydration activity. The acetone/propylene indicator shows it very clearly (Fig. 4).

Generally, isopropanol gets decomposed by two parallel reactions: dehydration to propene and/or diisopropyl ether on acidic-type centers and dehydrogenation to acetone on basic centers. Propene formation is correlated not only with the quantity of acidic sites but with their quality as well. The Brønsted acidity may play an important role in propene formation, but dehydration to propene proceeds also via isopropoxide species on strong Lewis acidic sites [18]. Over pure tin oxide, besides dehydrogenation, dehydration to diisopropyl ether and propene also takes place. After doping of tin oxide with cerium and rhodium, dehydrogenation activity decreases but propene is still present among the reaction products. The likely reason for the persistence of propene in the reaction products is the presence of the Lewis acid centers on the dehydrogenating

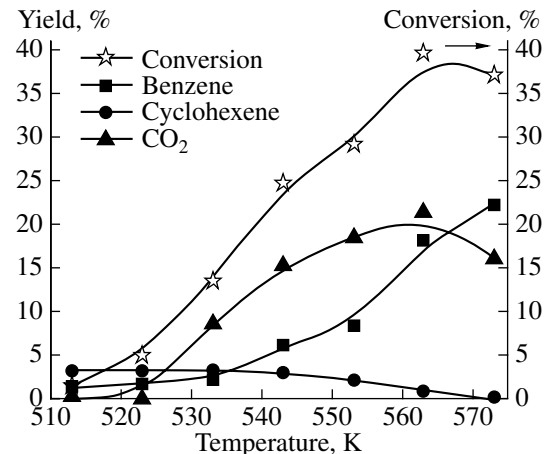


**Fig. 5.** Total conversion and yields of the products of the oxidative dehydrogenation of the cyclohexane versus  $\text{Sn}_{0.925}\text{Ce}_{0.07}\text{Rh}_{0.005}\text{O}_2$ .

$\text{Sn}_{0.925}\text{Ce}_{0.07}\text{Rh}_{0.005}\text{O}_2$  catalyst surface. The dehydration over both samples may also proceed via the route of the ElcB mechanism, which occurs characteristically on basic oxides. The mechanism is known to be associated with dehydrogenation [19]. Furthermore, the presence of cerium causes a greater basic character to the atoms next to the alcohol adsorbed, rendering the abstraction of the proton in the rate-determining step easier, thus increasing the rate of the reaction [20, 21].

### 3.4. Cyclohexane Test

Both catalysts were nearly catalytically inactive in the dehydrogenation of cyclohexane under nonoxidative conditions. Only traces of benzene in the investigated range of temperature were observed. Saturated hydrocarbon is much more reluctant to dehydrogenation than alcohol. When the carrier gas (helium) was replaced by air, the products appeared immediately. The results of the catalytic tests indicate that the  $\text{Sn}_{0.925}\text{Ce}_{0.07}\text{Rh}_{0.005}\text{O}_2$  catalyst effectively catalyzes oxidative dehydrogenation of cyclohexane into benzene, water, and cyclohexene (traces) at the investigated range of temperature, as well as total oxidation to carbon dioxide (Fig. 5). In addition, above 560 K, thermal decomposition of cyclohexane into small volatile products occurs. In contrast to the  $\text{Sn}_{0.925}\text{Ce}_{0.07}\text{Rh}_{0.005}\text{O}_2$  catalyst, the  $\text{SnO}_2$  sample demonstrates very low catalytic activity. The very low activity level in anaerobic conditions indicates that the reaction requires the presence of oxygen in the gas phase. It seems that the high catalytic activity of the doped tin dioxide sample results from the oxygen excess in the single-phase Sn-Ce-Rh-O due to the presence of the variable valence dopants. As suggested [2], chemisorption of oxygen on this material may induce holes in the rhodium *d*-band. When the hole is captured by the surface oxygen ion, its bonding to the surface is weakened and it can bond strongly to an

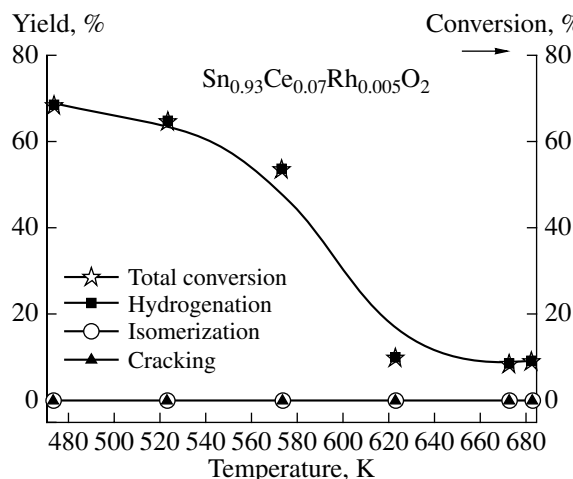


**Fig. 6.** Conversion and yield of the cyclohexene + H<sub>2</sub> versus Sn<sub>0.925</sub>Ce<sub>0.07</sub>Rh<sub>0.005</sub>O<sub>2</sub> test.

adsorbate [2, 22]. The consumed oxygen species can be subsequently regenerated by adsorption of oxygen from the gaseous phase. It has been shown that such surface oxygen species are very active in oxidation reactions [22]. In addition, hydrocarbon oxidation may be facilitated by the presence of Lewis acid centers, which may activate hydrocarbon [23–27]. The ability of Lewis acid sites to activate the ODH reaction of alkanes is in agreement with that found for other metal oxide-based catalysts [25–27]. It was established that the oxidative dehydrogenation of alkanes requires the presence of active sites of the Lewis base as well as of the Lewis acid character [25–28]. Accordingly, the role of acid sites was emphasized either for the oxydehydrogenation itself [15–27, 29] or for the formation of active coke on the catalyst surface where the process is properly developed [30]. Similarly, the same system V–Mg–O is active and selective in oxidative dehydrogenation of alkylaromatic hydrocarbons [31] and certain alcohols [32, 33].

### 3.5. Cyclohexene + H<sub>2</sub> Test

Taking into account the results of the catalytic tests presented, it was induced that the Sn<sub>0.925</sub>Ce<sub>0.07</sub>Rh<sub>0.005</sub>O<sub>2</sub> system would also selectively catalyze the hydrogenation of cyclohexene. The following reactions may proceed simultaneously: hydrogenation, isomerization to the five-membered ring, and opening of the ring and cracking. However, products of isomerization (methylcyclopentene) and cracking (hexene) were not found. Skeletal isomerization of cyclohexene and cracking proceed only on the catalysts with strong acid centers [34]. The reaction started with a cyclohexane yield exceeding 68% for 470 K (with the initial reaction rate  $6.8 \times 10^{-9}$  mol m<sup>-2</sup> s<sup>-1</sup>). But along with the temperature increase, the conversion decreased, as a result of the catalyst reduction (Fig. 6). The observed decrease of

conversion is caused by low stability of the catalyst under extreme reducing conditions. In such an atmosphere, this single-phased catalyst transforms to the material containing the white tin [35]. This process may be completely reversible. Partially reduced material, having been heated at ~870 K in ambient atmosphere, retrieves its microstructure with catalytic properties.

The results of the research performed have shown that the Sn<sub>0.925</sub>Ce<sub>0.07</sub>Rh<sub>0.005</sub>O<sub>2</sub> catalyst in normal operating conditions, i.e. in the course of bimolecular primary alcohol condensation and hydroxyarene alkylation with alcohols, keeps its catalytic parameters during long-lasting tests. It also reveals very good reproducibility. The level of conversion and the yield of the desired products remain the same after stopping the process and repeating the experiment. Although the molecular oxygen is not supplied with alcohol, the catalyst surface could get enriched in oxygen originating from the substrate. It could be the result of several consecutive conversions of aldehydes [36]. The molecules containing oxygen can also undergo decarbonization and dehydrogenation, even over dehydrogenating catalysts.

## CONCLUSION

The results of isopropanol and cyclohexane tests confirm the high dehydrogenating catalytic activity of the Sn<sub>0.925</sub>Ce<sub>0.07</sub>Rh<sub>0.005</sub>O<sub>2</sub> gas-sensitive material. They are coherent with the basic character; however, TPD have shown high total acidity (0.274 mmol/g) and the ammonia desorption versus temperature chart points to the high strength of the acid centers. The IR investigations performed with pyridine revealed the presence of the Lewis acid centers (0.126 mmol Py/g). The authors would point to the presence of these centers on the surface of the dehydrogenating catalysts as the factor providing the ability to catalyze the bimolecular condensation of aldehydes as well as the isopropanol dehydrogenation and oxydehydrogenation of cyclohexane. Thus, both the course of the bimolecular condensation of primary alcohols to ketones and the high yield of hydroxyarenes C-alkylation with alcohols are caused by the presence of the Lewis acid centers on the surface of the dehydrogenating Sn<sub>0.925</sub>Ce<sub>0.07</sub>Rh<sub>0.005</sub>O<sub>2</sub> catalyst. This property distinguishes the developed material from typical dehydrogenating catalysts, controlling the transformation of primary alcohols to aldehydes.

## REFERENCES

1. Polish Patent 183511, 1997.
2. Licznerski, B.W., Nitsch, K., Teterycz, H., and Wisniewski, K., *Sens. Actuators, B*, 2001, vol. 79, p. 157.
3. Motak, M., Samojeden, B., Teterycz, H., and Klimkiewicz, R., *XXXVIII Ogólnopolskie Kolokwium Katalityczne*, Krakow, 2006, PII-61, p. 312.

4. *Proc. Int. Symp. on Acid–Base Catalysis*, Tanabe, K., Hattori, H., Yamaguchi, T., and Tanaka, T., Eds., Sapporo, 1988.
5. Teterycz, H., Klimkiewicz, R., and Licznerski, B.W., *Appl. Catal.*, A, 2001, vol. 214, p. 243.
6. Klimkiewicz, R., Grabowska, H., and Teterycz, H., *Appl. Catal.*, A, 2003, vol. 246, p. 125.
7. Sato, S., Takahashi, R., Sodesawa, T., Matsumoto, K., and Kamimura, Y., *J. Catal.*, 1999, vol. 184, p. 180.
8. Klimkiewicz, R., Grabowska, H., and Syper, L., *Res. Chem. Intermed.*, 2003, vol. 29, p. 83.
9. Klimkevich, R., Grabovska, Kh., and Syper, L., *Kinet. Katal.*, 2003, vol. 44, no. 2, p. 307 [*Kinet. Catal.* (Engl. Transl.), vol. 44, no. 2, p. 283].
10. Klimkiewicz, R., Teterycz, H., Grabowska, H., Morawski, I., Syper, L., and Licznerski, B.W., *J. Am. Oil Chem. Soc.*, 2001, vol. 78, p. 533.
11. Honore, M., Lenaerts, S., Desmet, J., Huyberechts, G., and Roggen, J., *Sens. Actuators*, B, 1994, vols. 18–9, p. 621.
12. Licznerski, B.W., Teterycz, H., and Nitsch, K., *Proc. 23rd Conf. of the International Electronics and Packaging Society, Poland Chapter*, Koszalin, 1999, p. 35.
13. Berteau, P. and Delmon, B., *Catal. Today*, 1989, vol. 5, p. 121.
14. Datka, J., *J. Chem. Soc., Faraday Trans.*, 1981, vol. 1, p. 2877.
15. Trovarelli, A., *Catal. Rev. Sci. Eng.*, 1996, vol. 38, no. 4, p. 439.
16. Vlaic, G., Fornasiero, P., Geremia, S., Kaspar, J., and Graziani, M., *J. Catal.*, 1997, vol. 168, p. 386.
17. Teterycz, H., Klimkiewicz, R., and Laniecki, M., *Appl. Catal.*, A, 2004, vol. 274, p. 49.
18. Toda, Y., Ohno, T., Hatayama, F., and Miyata, H., *Appl. Catal.*, A, 2001, vol. 207, p. 273.
19. Molnár Á. and Bartók, M., in *Fine Chemicals through Heterogeneous Catalysis*, Sheldon, R.A. and van Bekkum, H., Eds., Weinheim: Wiley–VCH, 2001, p. 295.
20. Bernal, S., Blanco, C., Garcia, R., Olivan, A.M., and Trillo, J.M., *J. Catal.*, 1981, vol. 71, p. 21.
21. Goncalves, F.M., Medeiros, P.R.S., and Appel, L.G., *Appl. Catal.*, A, 2001, vol. 208, p. 265.
22. Morrison, S.R., *Catal. Sci. Technol.*, 1982, vol. 3, p. 199.
23. Ai, M., *J. Catal.*, 1977, vol. 49, p. 305.
24. Schuster, W., Niederer, J.P.M., and Hoelderich, W.F., *Appl. Catal.*, A, 2001, vol. 209, p. 131.
25. Vedrine, J.C., Millet, J.M.M., and Volta, J-C., *Catal. Today*, 1996, vol. 32, p. 115.
26. Busca, G., Finocchio, E., Ramis, G., and Ricchiardi, G., *Catal. Today*, 1996, vol. 32, p. 133.
27. Pantazidis, A., Auroux, A., Herrmann, J-M., and Mirodatos, C., *Catal. Today*, 1996, vol. 32, p. 81.
28. Bautista, F.M., Campelo, J.M., Garcia, A., Luna, D., and Marinas, J.M., *J. Catal.*, 1989, vol. 116, p. 338.
29. Tagawa, T., Iwayama, K., Ishida, Y., Hattori, T., and Murakami, Y., *J. Catal.*, 1983, vol. 79, p. 47.
30. Schraut, A., Emig, G., and Sockel, H.G., *Appl. Catal.*, 1987, vol. 29, p. 311.
31. Belomestnykh, I.P., Skrigan, E.A., and Isagulants, G.V., *Stud. Surf. Sci. Catal.*, 1992, vol. 72, p. 256.
32. Isagulants, G.V. and Belomestnykh, I.P., *Stud. Surf. Sci. Catal.*, 1996, vol. 108, p. 415.
33. Isagulants, G.V. and Belomestnykh, I.P., *Catal. Today*, 2005, vol. 100, p. 441.
34. Irvine, E.A., John, C.S., Kemball, C., Pearman, A.J., Day, M.A., and Sampson, R.J., *J. Catal.*, 1980, vol. 61, p. 326.
35. Teterycz, H., Klimkiewicz, R., Licznerski, B.W., and Kocemba, I., *Proc. 26th Int. Spring Seminar on Electronics Technology*, High Tatras, Slovak Republic, 2003, p. 375.
36. Klimkiewicz, R. and Drag, E.B., *J. Phys. Chem. Solids*, 2004, vol. 65, p. 459.